Elucidating the Therapeutic Potential of Cell-Penetrating Peptides in Human Tenon Fibroblast Cells

Amit Chatterjee, Samdani Ansar, Divya Gopal, Umashankar Vetrivel, Ronnie George, and Janakiraman Narayanan*
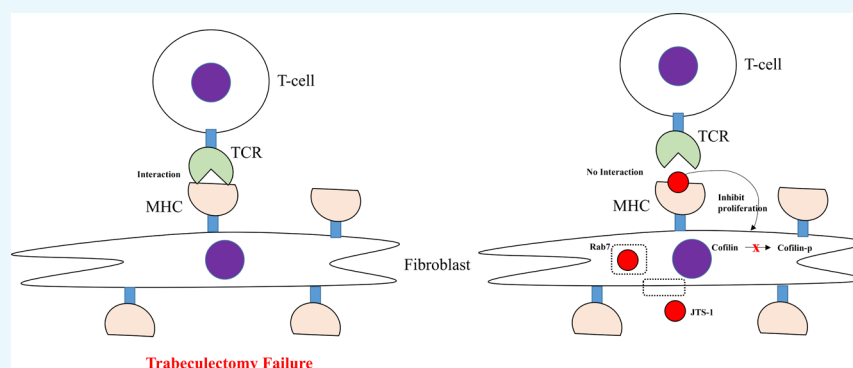
Read Online

ACCESS | Metrics & More | Article Recommendations | Supporting Information

ABSTRACT: Cell-penetrating peptides (CPPs) have been widely used as vehicles for delivering therapeutic molecules to the site of action. Apart from their delivering potential, the biological effects of CPPs have not been explored in detail. JTS-1 is a CPP that has been reported to have gene delivery functions, although its biological role is yet to be determined. Hence, in this study, we revealed the biological mechanism such as its uptake mechanism and immunogenic potential and function using primary human tenon fibroblast (TF) cells collected from patients undergoing glaucoma trabeculectomy surgery. Our results showed that the JTS-1 peptide has an α-helical structure and is nontoxic up to 1 μM concentration. It was found to be colocalized with early endosome (Rab5), recycling endosome (Rab7), and Rab11 and interacted with major histocompatibility complex (MHC) class I and II. The peptide also affected actin polymerization, which is regulated by cofilin phosphorylation and ROCK1 localization. It also inhibited TF cell proliferation. Therefore, the JTS-1 peptide could be used as a possible therapeutic agent for modifying the fibrosis process, where TF proliferation is a key cause of surgery failure.

1. INTRODUCTION

Cell-penetrating peptides (CPPs) like transactivator of transcription (TAT), penetratin, polyarginine, and MPG are being explored for delivering drug molecules to the target site in various ways.[1] They exhibit therapeutic functions like antifungal activity, in addition to being a delivery vehicle.[2,3] Several CPPs such as pexiganan, omiganan, PXLO1, and PAC-113 are in clinical trials for antimicrobial activity.[4,5] The outcome of the clinical trials depends on their stability, metabolic activity, bioavailability, enzymatic degradation, and the environment regulating the activity.[6] Delivery systems such as hydrogels, fibers, nanoparticles, etc.[7] address all of the above factors to improve the clinical outcome. However, the biological function of most CPPs was not explored in detail, which may influence the clinical outcome. A well-known CPP, for example, the TAT peptide, was explored for its biological function by Fotin-Mleczek et al. and found to internalize tumor necrosis factor (TNF) receptors, possibly through clathrin-dependent endocytosis[8] in HeLa cells. Moschos et al. found that the intratracheal administration of the TAT peptide

caused a significant reduction in p38 MAPK mRNA expression in mice.[9] Ekokoski et al. demonstrated that TAT is a potent inhibitor of PKC-α and PKC-β.[10] More than 70 kinases were found to be inhibited by TAT.[11] Hence, it is essential to understand the biological function of CPPs to reduce the off-target effects when using them as a carrier molecule before clinical trials.

Interestingly, the JTS-1 peptide was designed to replace viral vectors for gene therapy applications similar to the TAT peptide.[12] This peptide has been reported to disrupt the endosomal function,[13] which is regulated by actin polymerization. The cellular processes like cell migration, proliferation,

extracellular matrix remodeling, etc., are regulated by actin polymerization. Moreover, cofilin phosphorylation is known to regulate actin polymerization,[14] and it is known to regulate the cell proliferation in fibroblasts.[15] Impairment in these processes may lead to several pathological conditions. One such condition is post-trabeculectomy surgery for glaucoma, where wound-healing modulation is required. The endosomal dysregulation was reported to be one of the causes of trabeculectomy surgery failure.[16] The treatment options include medicines or surgery to lower the intraocular pressure.[17] Trabeculectomy surgery failure depends on the formation of a scar due to the difference in the conjunctival wound-healing response or due to the inflammation induced by the drugs.[18] Tenon fibroblast (TF) cells are reported to be the primary factor for initiating wound healing and scar formation post trabeculectomy.[19] The scar formation due to differentiation of fibroblasts into myofibroblasts results in extracellular matrix remodeling. Cytokines secreted by fibroblast cells drive the tenon fibrosis event post trabeculectomy.[20] Among various cytokines, the transforming growth factor (TGF)-β plays a crucial role in fibrosis. It causes the activation and proliferation of resident fibroblasts, as well as their migration into damaged tissues.[21] The abnormal interactions between fibroblasts and immune cells have been reported to contribute to the pathogenesis of aggressive wound healing.[22]

Mitomycin C (MMC) and 5-fluorouracil are being used to attenuate the subconjunctival fibroblast proliferation post trabeculectomy.[23] These drugs improved the success rate of trabeculectomy.[24] Brimonidine, a highly selective α_2 adrenergic agonist, is used for its putative antifibrotic role.[25] In 2014, ripasudil, a ROCK inhibitor, was approved in Japan for the treatment of ocular hypertension and glaucoma.[26] However, these drugs are toxic and can lead to further complications, such as subconjunctival bleb thinning, followed by leakage, cytotoxicity, and effects on neighboring ocular tissues.[27] Hence, there is a need to look for alternatives. The potential of CPPs to be used for the failure of trabeculectomy surgery has not been explored. Thus, we wanted to elucidate the potential role of the JTS-1 peptide as a therapeutic molecule if it can find a role in modulating the fibrosis process, which is a major concern post trabeculectomy surgery. In this study, we characterized the previously designed CPP JTS-1 and studied its uptake mechanism and interaction potential with MHC class I and II. We also elucidated its antiproliferative effect on TF cells and its mechanism of regulating signaling.

2. MATERIALS AND METHODS

2.1. Peptide Synthesis. Peptide JTS-1 (GLFEALLEL-LESLWELLLEA) was synthesized by solid-state synthesis and procured from M/s GenScript (https://www.genscript.com/) with an HPLC purity of more than 95%. The N terminal of the peptide was labeled with fluorescein isothiocyanate (FITC).

2.2. Structural Analysis of Peptides. The structure of JTS-1 was analyzed by circular dichroism (CD) spectroscopy, and the spectrum was recorded on a spectropolarimeter (J810; JASCO International Co., Ltd., Tokyo, Japan) using a 0.1 cm path length quartz cuvette at 37 °C. Spectra were recorded at two different temperatures (4 and 37 °C) at a scan rate of 50 nm/min.

2.3. Peptide Uptake and Toxicity Assay on Human TF Cells. This study, which is in accordance with the tenets of the Declaration of Helsinki, was reviewed by the local ethics

committee and approved by the institutional review board of Vision Research Foundation, Chennai, India (Ethics No. 635-2017). The tissues used for primary cell culture in this study were obtained from patients undergoing glaucoma trabeculectomy surgery after obtaining their signature and informed consent.

The primary human TFs cells were isolated from the tissue excised post sub-Tenon capsule trabeculectomy surgery. The cells were maintained in DMEM-F12 (Gibco, Life Technologies) with 20% FBS (fetal bovine serum, Gibco Life Technologies) and 1% antibiotics (Anti-anti, Gibco Life Technologies) in a 5% CO_2 incubator. The primary TF cells were characterized using the surface marker Vimentin. All of the experiments, including peptide uptake experiments, were done within four passages. The stock solution of the JTS-1 peptide was dissolved in distilled water at a stock concentration of 1 mM. TF cells were serum-starved for 24 h and then treated with two different concentrations (1 and 10 μM) of peptide for 24 h without fixation, and cell viability was assessed by the MTT assay using manufacturer's protocol. The JTS-1 peptide (1 μM) was incubated with TF cells to study the intracellular localization. Post 1 h of incubation, the cells were washed with phosphate-buffered saline (PBS) and visualized by fluorescence microscopy (Axio Observer, ZEISS GmbH, Germany, 100× oil immersion lens) using a FITC filter. Interleukin 6 (PeproTech, Cat No.-200-06) was procured, and concentrations of 0.1 ng/mL were used for TF cell treatment, which corresponds to a specific activity of $\geq 1 \times 10^7$ units/mg for 1 h.

2.4. Peptide Colocalization and Immunofluorescence. Primary TF cells were treated with 1 μM peptide for 1 h. Colocalization studies were performed with endocytic markers by fixing the cells with 4% paraformaldehyde and permeabilizing with 0.5% Triton X-100, followed by washing with 1× phosphate-buffered saline (PBS). Blocking was performed using 1% bovine serum albumin (BSA) before overnight incubation with primary antibody, EEA, clathrin, Rab5, Rab7, and Rab11, ROCK1, and phalloidin (Cat. No. Endosomal Marker sampler kit Actin stain-488 cytoskeleton). The detection was done using Cy3.5 secondary antibody and counterstained with Hoechst (Thermo Fisher Cat. No. 33342).

2.4.1. Statistical Analysis. All experiments were performed on at least three independent samples. Paired Student's "t" test was performed on at least three experiments. The samples are stained with primary antibody and counterstained with Hoechst (Thermo Fisher Cat. No. 33342). P values were <0.05, 0.01, and 0.001.

2.5. Peptide Interaction Prediction. *2.5.1. Cytotoxic T-Lymphocyte (CTL) Epitope Prediction. 2.5.1.1. MHC I Binding Production.* The CTL epitopes spanning the peptides were predicted using the NetCTL 1.2 server (http://www.cbs.dtu.dk/services/NetCTL/).[28] This server uses a weight matrix and an artificial neural network for the prediction of the class I MHC binding affinity, TAP (transport associated with antigen processing) transport efficiency, and proteosomal C-terminal cleavage activity. The server uses 12 MHC class I subtypes for prediction: HLA-A*01:01 (A1), HLA-A*02:01 (A2), HLA-A*03:01 (A3), HLA-A*24:02 (A24), HLA-A*26:01 (A26), HLA-B*07:02 (B7), HLA-B*08:01 (B8), HLA-B*27:05 (B27), HLA-B*39:01 (B39), HLA-B*40:01 (B44), HLA-B*58:01 (B58), and HLA-B*15:01 (B62).
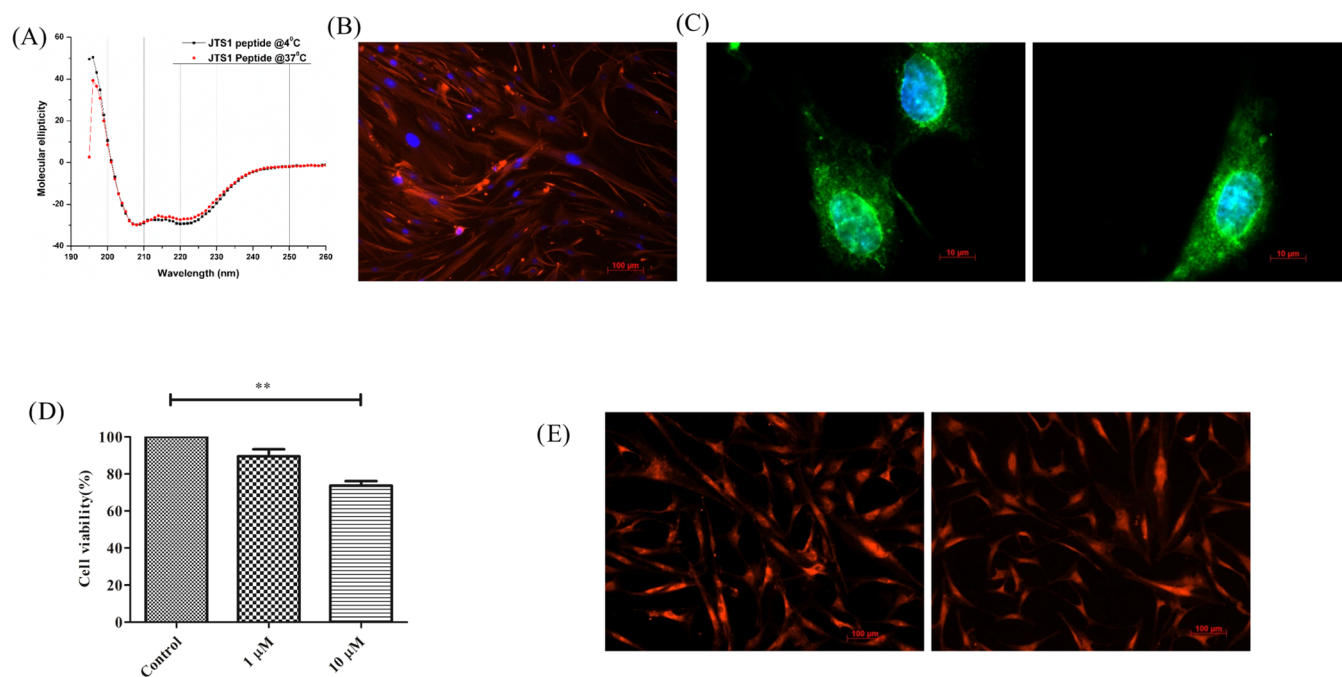
Figure 1. Peptide structure and uptake: (A) CD spectra of the JTS-1 peptide at 37 and 4 °C; (B) vimentin marker expression in TF cells; (C) uptake of the JTS-1 peptide at 1 and 24 h without fixation in TF cells; (D) MTT assay of the JTS-1 peptide at two concentrations; (E) MitoTracker staining of JTS-1-treated cells (at 1 μM concentration) and the untreated control.

2.5.1.2. MHC II Binding Prediction. The NetMHCII 2.3 server (http://www.cbs.dtu.dk/services/NetMHCII/)[29] was used for the prediction of the possible epitopes that can bind with class II MHC alleles. The NetMHCII uses artificial neural networks, which are trained using the already known MHC II binding peptides for the prediction of MHC II binding peptides. The binding prediction was done for the 25 HLA-DR alleles, 20 HLA-DQ, and 9 HLA-DP alone.

2.5.1.3. Peptide Docking with MHC I and MHC II. The MHC I and II alleles that bind to the epitope region were predicted (sequence-based) and collected. The allele structures corresponding to the respective MHC class I and II were downloaded from the pHLA3D database (https://www.phla3d.com.br/alleles/index).[30] The pHLA3D database contains modeled three-dimensional (3D) structures of the HLA proteins for a wide range of HLA alleles. The protein structures available in pHLA3D are modeled using Modeller with a similar identity containing the template HLA structure from PDB. The modeled structures are refined using Galaxy Refine, followed by structural quality assessment such as Ramachandran plot, PROCHECK, and ERRAT. The predicted epitopes from the sequence analysis for MHC I and MHC II binding were subjected to the peptide docking with their respective predicted alleles using the HPEPDOCK server (http://huanglab.phys.hust.edu.cn/hpepdock/).[31] The HPEPDOCK server will model the peptide structure from the sequence using MODPEP (peptide structure prediction tool) with 1000 conformers per peptide with the secondary structure of the peptide, as predicted using the PSI-PRED. The 1000 conformers for each peptide were docked against the respective allele structures and ranked in accordance with the docking score, wherein the lowest score will have the highest binding affinity. The HPEPDOCK is also shown to outperform other docking tools for predicting the peptide pose in the previous benchmarking studies.[32]

2.6. RNA Extraction and Quantitative Polymerase Chain Reaction (qPCR). The primary TF cells were treated with 1 μM JTS-1 peptide for 1 h, and total RNA was extracted using the Trizol method according to the manufacturer's protocol (Sigma-Aldrich). The total RNA concentration was determined using a BioSpec-nano spectrophotometer (Shimadzu). cDNA was synthesized using the iScript cDNA conversion kit (Bio-Rad). Quantitative real-time PCR was performed using an Applied Biosystems 7300 with SYBR Green chemistry (Applied Biosystem). The primer details are mentioned below:

primer name	primer sequence
IL-6-F	5′-GCAGAAAAAGGCAAAGAATC-3′
IL-6-R	5′-CTACATTTGCCGAAGAGC-3′
TGFB1-F	5′-TGTACCAGAAATACAGCAAC-3′
TGFB1-R	5′-CAAAAGATAACCACTCTGGC-3′
MMP-2-F	5′-GCCAATGATCCTGTATGTG-3′
MMP-2-R	5′-GTGATCTTGACCAGAATACC-3′
MMP-13-F	5′-AGGTAGAAAATTTTGGGCTC-3′
MMP-13-R	5′-CTTAACTTCTTTTGGAAGACCC-3′
IL-8-F	5′-GTTTTTGAAGAGGGCTGAG-3′
IL-8-R	5′-TTTGCTTGAAGTTTCACTGG-3′
ACTB-F	5′-GACGACATGGAGAAAATCT-3′
ACTB-R	5′-ATGATCTGGGTCATCTTCTC-3′

2.7. Immunoblotting. After 1 h of incubation with 1 M JTS-1 peptide, the cells were collected, and lysates were prepared using the radioimmunoprecipitation (RIPA) assay buffer (EMD 340 Millipore Cat. No. 20-188) as specified by the manufacturer for Western blotting. In the electrophoresis chamber, an equal concentration of tissue lysate was loaded and separated on a sodium dodecyl sulfate polyacrylamide gel (SDS-PAGE) at 100 V (25 mM Tris, 190 mM glycine, and 0.1 % SDS). Proteins were isolated and transferred to poly-(vinylidene difluoride) (PVDF) membranes, which were then blocked for 1 h at 37 °C in TBST containing 5% (w/v) nonfat
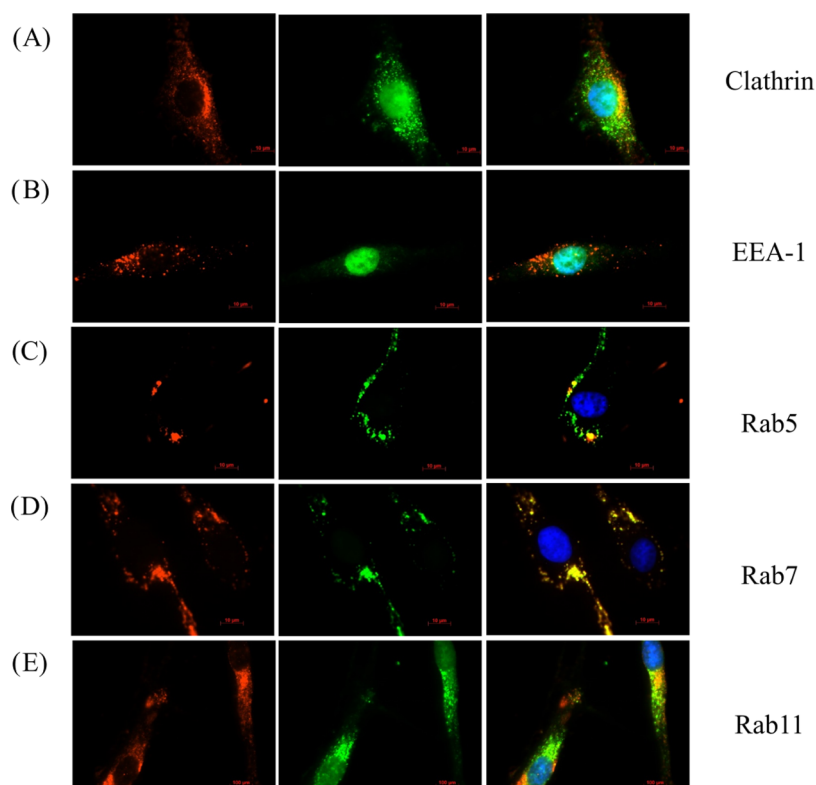
Figure 2. Mechanism of peptide uptake in TF cells: the JTS-1 peptide colocalization with antibodies of (A) clathrin heavy chain, (B) early endosomal antigen, (C) Rab5, (D) Rab7, and (E) Rab11.

dry milk powder (NFDM) (20 mM Tris-HCl pH 7.5, 150 mM NaCl, and 0.1 % Tween 20). It was rinsed with TBST and treated overnight at 4 °C with antibodies like phospho-cofilin, cofilin, paxillin, ROCK1 (CST Cat. No. 12,666, CST Cat. No. 9967, CST Cat. Nos. 2542, and ab245368 we) phospho p44 and p44. Student's *t*-test was performed for all of the data to obtain the statistical significance, where * represents $P < 0.5$ and ** represents $P < 0.05$. Immunoblotting experiments were done in $n = 4$ samples.

2.8. BrdU Cell Proliferation Assay. BrdU (Roche cell proliferation ELISA kit) reagent was used to assess cellular proliferation. The primary TF cells were planted at a density of 10,000 cells per well in a 12-well plate and grown overnight to monitor cell proliferation. A peptide treatment of 1 and 10 M was given for 24 h, followed by 2 h of BrdU incubation, 30 min of fixation, and 90 min of incubation with anti-BrdU. After adding a chromogenic substrate, the color intensity was evaluated by spectrophotometry. Both control and peptide-treated cells were subjected to a BrdU test. The absorbance of peptide-treated cells was subtracted from the absorbance of untreated cells as a control. By subtracting untreated cells from 100 %, the percentage of cellular proliferation in each peptide concentration was calculated. Graphpad Prism software was used to create the percentage bar graph.

3. RESULTS

3.1. Peptide Structure Characterization and Uptake Studies. To test the effect of temperature, we confirmed the secondary structure of peptides using CD spectra at two different temperatures, 37 and 4 °C. The results (Figure 1A) showed that at 4 °C, the JTS-1 peptide exhibited negative absorption at 222 and 208 nm and positive absorption at 195

Table 1. Predicted CTL Epitopes from Peptides Using NetCTL 1.2 with the Combined Score and the Corresponding Peptide Docking Score Value from HPEPDOCK

MHC I allele	peptide sequence	combined score	docking score
HLA-A*02:01 (A2)	GLFEALLEL	1.4312	−184.797
	ALLELLESL	1.372	−179.071
	SLWELLLEA	1.3156	−207.55
	ELLESLWEL	1.1981	−181.2
HLA-A*26:01 (A26)	ELLESLWEL	1.0475	−152.481
HLA-B*39:01 (B39)	LESLWELLL	0.9176	−243.254
HLA-B*40:01 (B44)	LESLWELLL	1.1611	−162.857
HLA-B*15:01 (B62)	GLFEALLEL	0.8541	−163.783

nm; however, at 37 °C, the absorbance at 195 nm diminished, while the helix structure remained. The findings revealed that the JTS-1 peptide could have an α-helical structure that did not change with temperature. It was also found to have a negative charge, as previously reported. This was also substantiated using zeta potential (Figure Supporting Data S2) data.

The tissue was obtained from patients undergoing trabeculectomy surgery. Human TFs cells were isolated from the tissue, and the fibroblast phenotype was confirmed by the expression of the surface protein marker vimentin (Figure 1B). The uptake of the JTS-1 peptide in TF cells was investigated at two time points: 1 and 24 h without fixation. The JTS-1 peptide was taken up within 1 h and remained stable for 24 h, as shown in Figure 1C. Surprisingly, the peptide JTS-1 was found in both the cytoplasm and the nucleus at both time points. Furthermore, we investigated the toxicity of peptides (using the MTT assay) at two different peptide concentrations
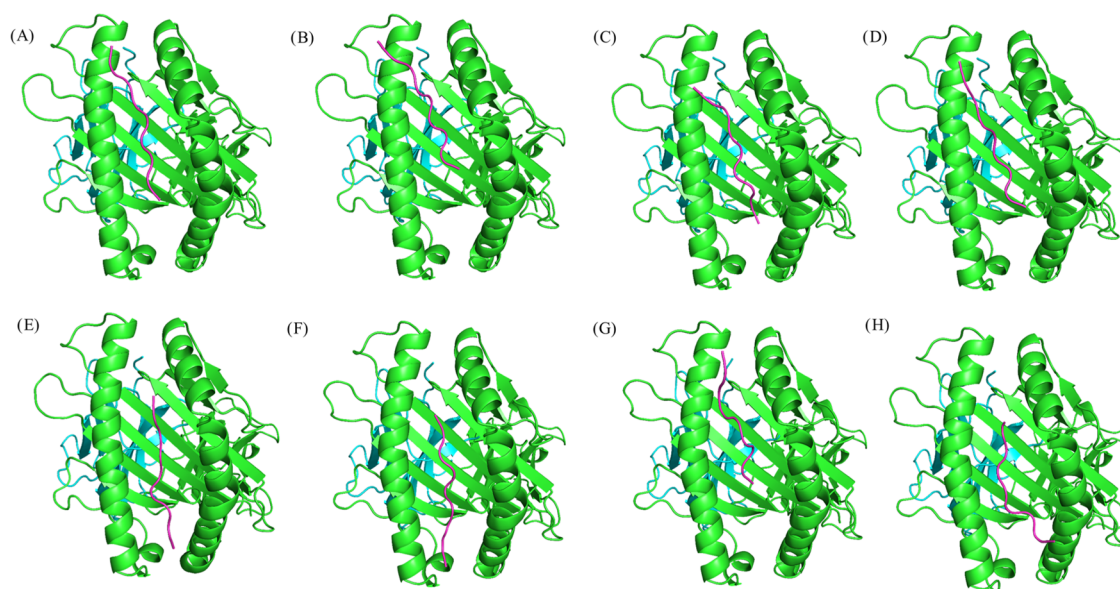
Figure 3. In silico JTS-1 peptide and MHC class I interaction: the class I MHC allele and the predicted epitopes are docked and shown as follows: (A) HLA-A*02:01(A2)-GLFEALLEL, (B) HLA-A*02:01(A2)-ALLELLESL, (C) HLA-A*02:01(A2)-SLWELLLEA, (D) HLA-A*02:01(A2)-ELLESLWEL, (E) HLA-A*26:01(A26)-ELLESLWEL, (F) HLA-B*39:01(B39)-LESLWELLL, (G) HLA-B*40:01(B44)-LESLWELLL, and (H) HLA-B*15:01(B62)-GLFEALLEL. A schematic illustration of the protein structure is shown, where the HLA α chain is represented in green color, β-2-microglobulin is represented in cyan color, and the predicted epitope is represented in magenta color. The figures were prepared using Pymol-2.2.1 (the PyMOL molecular graphics system, version 2.2.1 Schrödinger, LLC).

Table 2. Predicted MHC II Epitopes from Peptide Using NetMHC-2.3 with Rank and the Corresponding Peptide Docking Score Value from HPEPDOCK

MHC II allele	peptide sequence	rank	docking score
HLA−DRB1_0404	EALLELLESLWELLL	1.9	−188.398
HLA−DPA10103-DPB10201	ALLELLESLWELLLE	0.25	−198.674
	EALLELLESLWELLL	0.25	−207.635
	FEALLELLESLWELL	0.25	−222.895
	GLFEALLELLESLWE	1.7	−237.212
	LFEALLELLESLWEL	1.1	−209.812
	LLELLESLWELLLEA	0.4	−187.201
HLA−DPA10103-DPB10401	ALLELLESLWELLLE	0.5	−224.613
	EALLELLESLWELLL	0.5	−217.327
	FEALLELLESLWELL	0.7	−260.417
	LLELLESLWELLLEA	0.5	−206.266
HLA−DPA10201-DPB10101	ALLELLESLWELLLE	0.9	−220.357
	LLELLESLWELLLEA	0.6	−202.89
HLA−DPA10301-DPB10402	ALLELLESLWELLLE	1	−197.615
	EALLELLESLWELLL	1.2	−216.699
	FEALLELLESLWELL	1.2	−247.78
	LLELLESLWELLLEA	0.6	−187.087
HLA−DQA10101-DQB10501	LLELLESLWELLLEA	1.9	−214.054

(1 and 10 μM) for 24 h. Strikingly, the peptide JTS-1 was found in both the cytoplasm and the nucleus at both time points. Furthermore, we probed the toxicity of peptides (using the MTT assay) at two different peptide concentrations (1 and 10 M) for 24 h. No significant toxicity was observed on treatment with 1 μM JTS-1 peptide, whereas at 10 μM concentration, only 80% of cells were viable, resulting in a 20% reduction (Figure 1D). Furthermore, the toxicity was validated by assessing the mitochondrial function in TF cells using MitoTracker (red dye). At 1 μM JTS-1 peptide concentration, no significant changes in the mitochondrial function were

observed (Figure 1E). All subsequent experiments were carried out at a concentration of 1 μM.

3.2. Uptake Mechanism of the JTS-1 Peptide. To properly appreciate how this pathway is regulated, we colocalized the JTS-1 peptide with clathrin, EEA1, Rab5, Rab7, and Rab11 (Figure 2A−E). The JTS-1 peptide partially colocalized with clathrin and EEA1, implying the involvement of multiple endocytic mechanisms in TF cells. Furthermore, the JTS-1 peptide colocalized with early endocytic vesicles (Rab5) and recycling endosomes (Rab11), indicating that the JTS-1 peptide managed to escape from early endocytic vesicles and recycling vesicles. However, the JTS-1 peptide completely colocalized with Rab7, indicating that the peptide was delivered both cytosolically and nuclearly. Rab11 is a recycling endosome marker that regulates the recycling of endocytosed proteins and peptides.[33] As a result of our findings, we may deduce that the JTS-1 peptide colocalized with Rab proteins and was transported to the cytosol and nucleus. Our findings showed that endocytosed peptides could be recycled back to the plasma membrane due to partial colocalization of the JTS-1 peptide with Rab11.

3.3. JTS-1 Interaction with the Major Histocompatibility Complex. We also used an online program (http://imed.med.ucm.es/Tools/antigenic.pl) to determine the antigenicity of the JTS-1 peptide. The predictions are based on the presence of amino acid residues in segmental epitopes that have been studied experimentally. The antigenicity of the JTS-1 peptide was found between positions 4 and 16 in a 20-amino-acid sequence (Figure S1). The JTS-1 peptide and partial colocalization with Rab11, a known interacting partner of MHC1 and MHC II, encouraged us to study the interaction potential of the peptide with both classes of proteins to see if it can generate antigenicity. Using the NetCTL 1.2 server, CTL epitopes from the peptide sequence (GLFEALLELLESL-WELLLEA) that can bind with class I MHC were identified. For the prediction, a weight of 0.15 for C-terminal cleavage, a
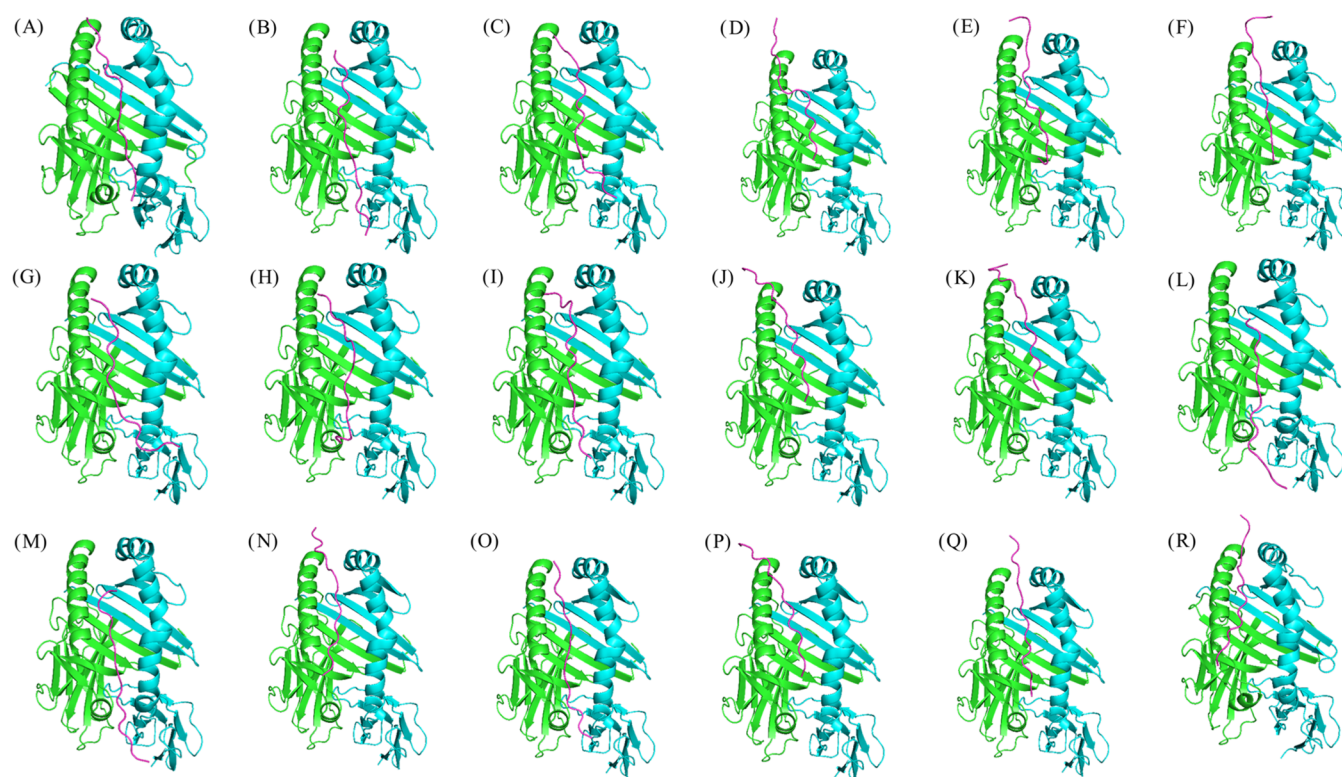
Figure 4. In silico JTS-1 peptide and MHC class II interaction: the class II MHC allele and the predicted epitope are docked and shown as follows: (A) HLA−DRB1_0404-EALLELLESLWELLL, (B) HLA−DPA10103-DPB10201-ALLELLESLWELLLE, (C) HLA−DPA10103-DPB10201-EALLELLESLWELLL, (D) HLA−DPA10103-DPB10201-FEALLELLESLWELL, (E) HLA−DPA10103-DPB10201-GLFEALLELLESLWE, (F) HLA−DPA10103-DPB10201-LFEALLELLESLWEL, (G) HLA−DPA10103-DPB10201-LLELLESLWELLLEA, (H) HLA−DPA10103-DPB10401-ALLELLESLWELLLE, (I) HLA−DPA10103-DPB10401-EALLELLESLWELLL, (J) HLA−DPA10103-DPB10401-FEALLELLESLWELL, (K) HLA−DPA10103-DPB10401-LLELLESLWELLLEA, (L) HLA−DPA10201-DPB10101-ALLELLESLWELLLE, (M) HLA−DPA10201-DPB10101-LLELLESLWELLLEA, (N) HLA−DPA10301-DPB10402-ALLELLESLWELLLE, (O) HLA−DPA10301-DPB10402-EALLELLESLWELLL, (P) HLA−DPA10301-DPB10402-FEALLELLESLWELL, (Q) HLA−DPA10301-DPB10402-LLELLESLWELLLEA, and (R) HLA−DQA10101-DQB10501-sLLELLESLWELLLEA. Schematic illustration of the protein structure is shown, where the HLA α chain is represented in green color, the HLA β chain is represented in cyan color, and the predicted epitope is represented in magenta color. The figures were constructed using Pymol-2.2.1 (the PyMOL molecular graphics system, version 2.2.1 Schrödinger, LLC).

weight of 0.05 for TAP transport efficiency, and a threshold of >0.75 for epitope identification were used. The server predicts each epitope (10 mer) for each allele and calculates the total score. This metric considers C-terminal cleavage, TAP transport efficiency, and MHC I binding affinity. Only epitopes with a combined score greater than 0.75 were considered for docking with MHC I alleles. Table 1 presents the class I HLA alleles and epitopes with the highest combined score. Using the HPEPDOCK server, the predicted epitopes were docked with the respective class I MHC allele structures. Table 1 shows the docking score of each peptide with the MHC I allele. The results (Table 1 and Figure 3) demonstrated that the predicted epitopes from the sequence could be docked into the MHC I alleles' epitope-binding groove with a high docking score. The predicted epitopes also had a higher number of hydrogen and hydrophobic interactions with MHC I allele epitope-binding groove residues (Table S1). This suggested that the predicted epitopes could bind to the MHC I allele and present the epitope region for a cytotoxic T-cell-mediated immune response.

The NetMHCII 2.3 server was also used to predict class II MHC binding epitopes. The server predicted various epitope regions with MHC II alleles of length 15 mer. The threshold for strong epitope binding was set at 2 (% Rank value), and the threshold for weak epitope binding was set at 10 (% Rank

value). Table 2 shows the predicted epitope sequence along with the associated alleles and Rank score. Furthermore, only the epitope with a strong binding score of <2 Rank was considered for peptide docking. The predicted epitopes were docked with the MHC II alleles using HPEPDOCK, and the docking score is shown in Table 2. The predicted epitopes docked well into the epitope-binding region groove in the structure of the respective MHC II allele (Figure 4) with a high docking score. A greater number of hydrogen and hydrophobic interactions were also observed between the predicted epitopes and the residues in the MHC II alleles' epitope-binding groove (Table S2). We conclude that the predicted epitope region of the peptide binds with MHC II alleles and has the potential to elicit an immune response.

3.4. Immunogenic Activity of the JTS-1 Peptide. Cytokine, growth factor, and extracellular matrix (ECM) modulator estimations are used to assess the putative immunomodulatory action anticipated by bioinformatics analysis. The primary TF cells were treated for 1 h with the JTS-1 peptide at a concentration of 1 μM. qPCR was used to assess the expression of cytokines such as IL-6, IL-8, TGF-β, MMP-13, and MMP-2 after treatment. The results (Figure 5A,B) showed that peptide-treated TF cells had a considerable ($P > 0.005$) elevation of IL-6 and IL-8. MMP-2 expression remained unchanged, whereas MMP-13 expression was
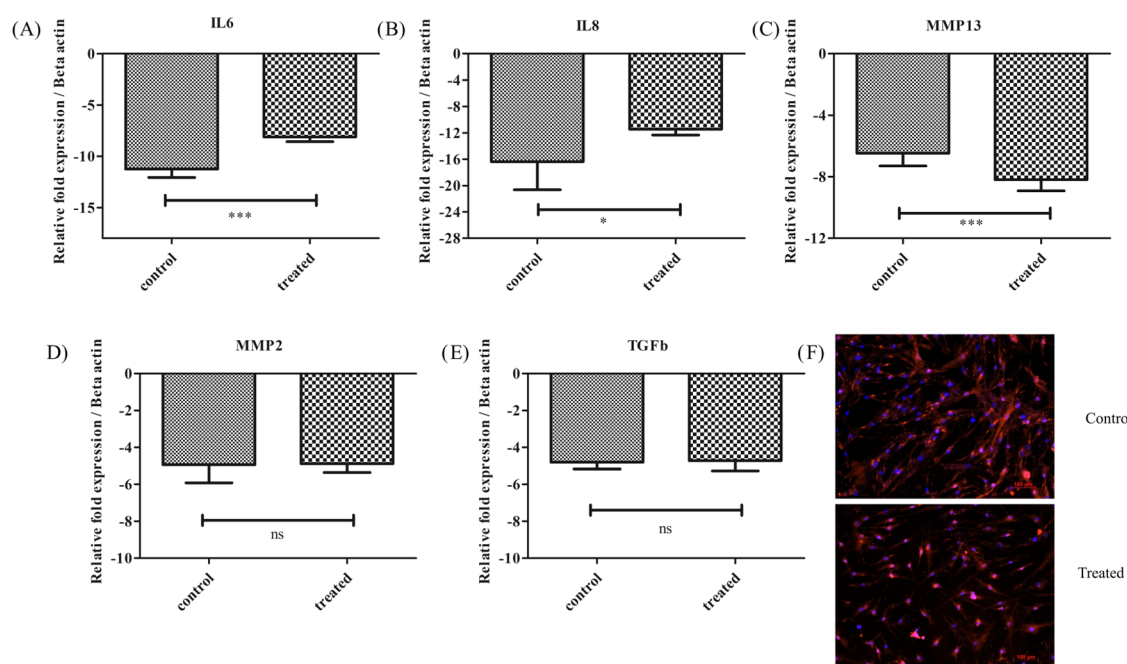
Figure 5. Peptide treatment on human tenon fibroblast (TF) cells and its effect on biological functions: RT PCR of various cytokine mRNA: (A) IL-6, (B) IL-8, (C) MMP-13, (D) MMP-2, and (E) TGF-β. (F) Immunofluorescence of TGF-β for peptide-treated and untreated TF cells.
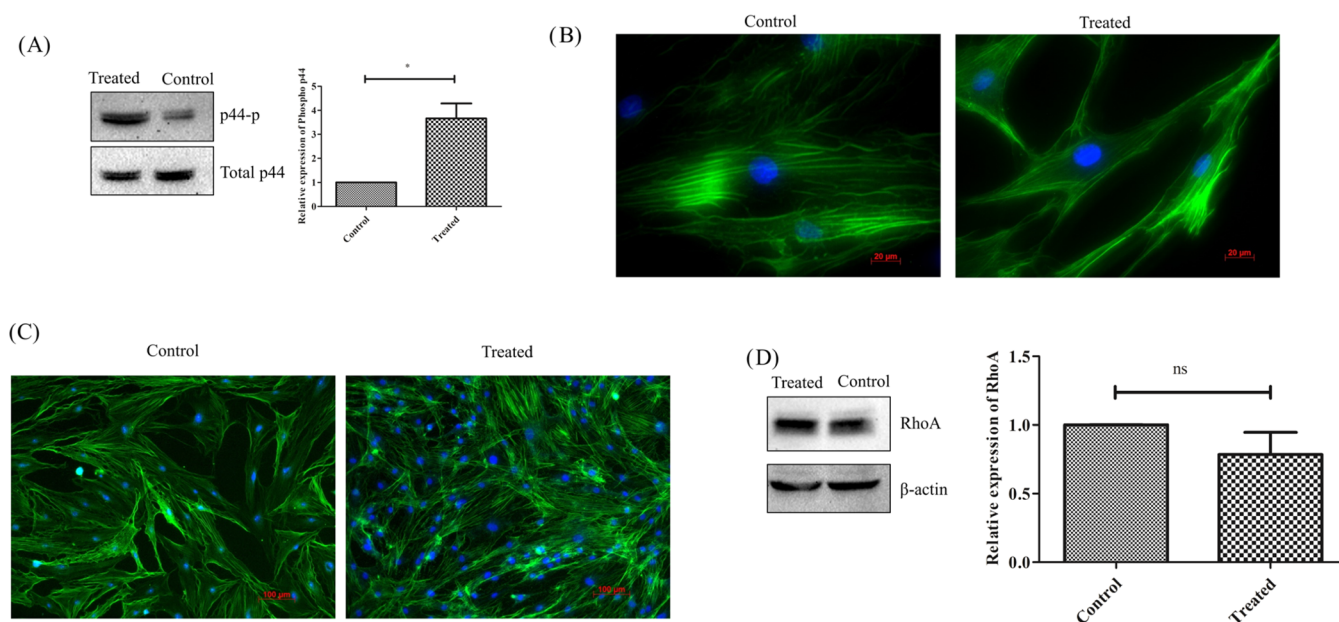

Figure 6. (A) Immunoblotting of phospho p44 in control and JTS-1 peptide-treated TF; (B) phalloidin staining of TF in control and IL-6-treated TF cells; (C) actin staining of TF in control and JTS-1-treated TF cells; and (D) immunoblotting of RhoA, in control and JTS-1 peptide-treated TF cells.

substantially ($P > 0.0005$) reduced (Figure 5C,D). TGF-mRNA expression in TF cells also exhibited no significant changes (Figure 5E). TGF-expression remained unchanged (Figure 5F) even after peptide treatment, which was similar to the level of mRNA expression. The JTS-1 peptide induced changes in cytokines such as IL-6, IL-8, and MMP-13, according to our findings. Furthermore, it is known that the p44 map kinase regulates the IL-6 family of cytokines independently of the JAK-STAT pathway. As a result, we investigated phospho p44 expression in TF cells following JTS-1 peptide treatment. Our findings revealed a significant ($P <$

0.05) increase in phospho p44, indicating that the JTS-1 peptide also regulates the MAP kinase pathway (Figure 6A). This study concludes that the JTS-1 peptide can induce cytokines such as IL-6 and IL-8 via the p44 pathway while maintaining TGF-β. These data are consistent with the in silico data of peptide binding to MHC1 and II to induce antigenicity.

3.5. Actin Remodeling Induced by the JTS-1 Peptide. To investigate the effect of cytokines, we treated the TF cells with recombinant IL-6 and observed the formation of stress fibers. We noticed that IL-6 treatment of TF cells resulted in the formation of stress fibers (Figure 6B), correlating with
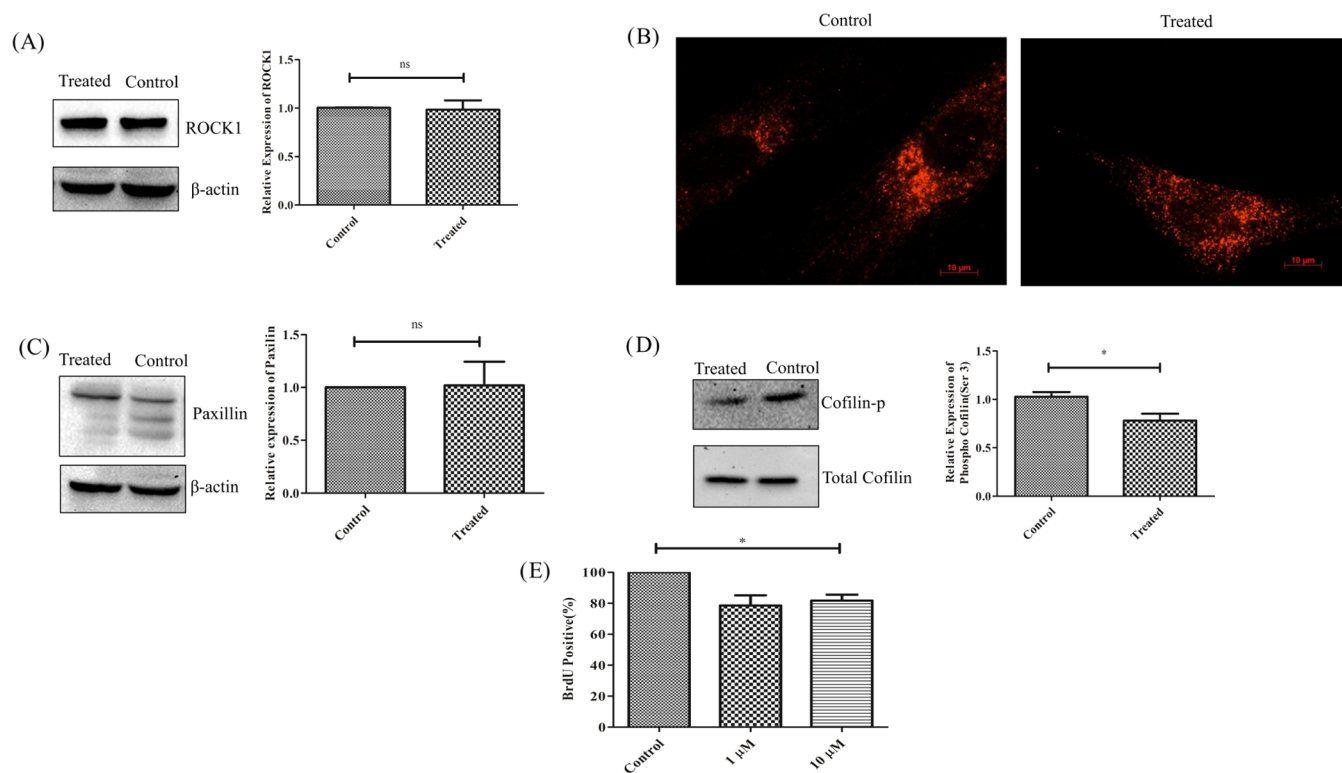
Figure 7. (A) Immunoblotting of ROCK1, in control and JTS-1 peptide-treated TF cells; (B) immunofluorescence of ROCK1 in control and JTS-1 peptide-treated TF cells; (C) immunoblotting of paxillin in control and JTS-1 peptide-treated TF cells; (D) immunoblotting of phospho-cofilin-treated TF cells; and (E) cell proliferation assay using BrdU in peptide-treated TF cells.

previous findings.[34] Similarly, we discovered that the JTS-1 peptide increased IL-6 expression in TF cells and caused a significant change in F-actin organization (Figure 6C). As a result, we investigated the expression of RhoA and ROCK1, a member of the serine/threonine-protein kinase family and an immediate downstream molecule of RhoA. Our findings revealed no significant changes in the expression of RhoA (Figure 6D) or ROCK1 (Figure 7A). However, we discovered ROCK1 nuclear localization in peptide-treated TF cells (Figure 7B), which warrants further investigation. We also looked at total paxillin and cofilin expression, which was found to be the same in both treated and control groups (Figure 7C,D). However, cofilin phosphorylation was significantly ($P >$ 0.05) reduced in JTS-1 peptide-treated TF cells (Figure 7D). Cofilin is an actin-depolymerizing protein whose function is negatively regulated by phosphorylation at the Ser3 residue. Using the BrdU assay, we also investigated the effect of the JTS-1 peptide on TF cell proliferation. Our findings showed that at 1 and 10 μM concentrations, there was a significant ($P > 0.05$) reduction in cell proliferation (Figure 7E). As a result, our findings indicate that the JTS-1 peptide had an α-helical structure and was taken up via multiple endocytic mechanisms. The JTS-1 peptide was discovered to be immunogenic and to alter cytokine expression. Furthermore, it decreased cofilin phosphorylation and actin polymerization, both of which affected TF cell proliferation.

4. DISCUSSION

The Trojan horse approach[35] has been used to describe CPP-mediated delivery of therapeutic molecules such as proteins, drugs, DNA, and siRNA. However, due to its off-target effect, this approach has recently been deemed unsuitable for in vivo

applications.[36] TNF-mediated signal transduction has been inhibited by cationic CPPs such as Antennapedia homeo-domain-derived peptide (Antp), non-arginine, and TAT-derived peptide.[8] Recent studies on CPPs have revealed that in addition to acting as delivery vehicles, these CPPs have been reported to modulate a variety of other signal transduction pathways, which require further investigation. To fill this gap in the field of CPP delivery, we investigated the effect of JTS-1 in TF cells. JTS-1 was designed with an α-helical structure to replace gene therapy viral vectors.[37] The JTS-1 peptide was designed to form a complex with DNA and demonstrated improved transfection in epithelial cell lines.[38] The peptide interacts spontaneously with DNA and disrupts the endosome, allowing for efficient gene transfer.[39] However, its biological function was unknown. As a result, in this study, we attempted to decipher its biological function using primary TF cells. We investigated the molecular mechanism of the JTS-1 peptide and its effect on TF cells to determine its potential application as an antifibrotic peptide. The molecular modeling of the peptide revealed an α-helical structure, which is in accordance with a previous report.[12] The predicted α-helical structure was validated by CD spectroscopy, which revealed no variation in the structure with temperature change. The peptide's charge was also revealed to be negative using zeta potential analysis. Furthermore, the JTS-1 peptide uptake was comparable to that of other CPPs[40,41] such as TAT and MK2 inhibitor peptides within 1 h. The JTS-1 peptide has been reported to disrupt the endosomes.[42] The Rab family of proteins are the key regulator of endosomal trafficking and remodeling.[43] Rab5, Rab7, and Rab11 are markers of early, late, and recycling endosomal pools, respectively.[44] Rab5 controls clathrin-mediated endocytosis from the plasma membrane to the pool of early/sorting

endosomes. The Rab5 effector protein early endocytic protein (EEA1) modulates membrane trafficking.[45] Our findings revealed perfect colocalization with multivesicle Rab7 but only partial colocalization with clathrin, early endosome (Rab5), and recycling endosome (Rab11). Rab7 has also been implicated in antigen presentation with class II molecules for a variety of peptide−MHC combinations.[46] In nonprofessional antigen-presenting cells, Rab5 EEA mediates the MHC class I recycling pathway.[47] The JTS-1 peptide may elude the endocytic machinery and present itself to Rab7 for antigen presentation, according to our findings. However, further research is needed to determine the precise process of antigen presentation.

Using an online program, we also discovered that the peptide has antigenic properties. The immunomodulatory role of the JTS-1 peptide, on the other hand, has not been investigated. We tested JTS-1 peptide binding to MHC I and II receptors in host cells to see if it plays a role in immunogenic regulation.[48] MHC I is expressed by all nucleated cells, whereas MHC II is expressed by only antigen-presenting cells.[49] Hence, we used an online prediction platform and peptide docking to examine the binding capability of JTS-1 peptide epitopes with both MHC class I and II alleles. The findings showed that the peptide interacts with and binds to the epitope-binding grooves of both MHC I and II. This suggests that the peptide could modify immunogenicity by regulating antigenicity through putative binding to both receptor proteins. The JTS-1 peptide influenced the expression of IL-6, IL-8, and MMP-13, demonstrating that it can induce cytokines. Rab11 has also been shown to increase antigenic peptide exchange in recycling endosomes and regulate MHC class II recycling.[50] Cytokines have been shown to cause F-actin reorganization in endothelial cells via RhoA activation.[34] As a result, we investigated the ability of JTS-1 peptides to induce cytokine responses in TF cells. JTS-1 significantly increased the expression of IL-6, IL-8, and MMP-13, according to our findings. Furthermore, the peptide treatment increased phospho p44 levels, indicating a role for this protein in cytokine response.[51] The peptide did not affect RhoA, ROCK1, or paxillin expression, but it did affect cofilin phosphorylation. Ripasudil, a Rho-kinase pathway signaling inhibitor, has been used successfully in clinics to control intraocular pressure in glaucoma patients.[52] However, its role in regulating TF proliferation is still being investigated.

Our findings suggest that the JTS-1 peptide has an α-helical structure, is immunogenic, and is rapidly absorbed. It promotes the expression of IL-6, which controls cofilin phosphorylation and the formation of actin stress fibers. As a result, by regulating actin polymerization, we can inhibit the proliferation of TF cells. However, one of the major disadvantages of such CPPs was the inhibitors' incomplete specificity to the target. Furthermore, animal studies on its stability and toxicity are required before it can be used as a therapeutic agent to modulate the fibrosis process.

ASSOCIATED CONTENT

ⓈⒾ Supporting Information

The Supporting Information is available free of charge at https://pubs.acs.org/doi/10.1021/acsomega.2c00701.

> JTS-1 peptide showing antigenicity in the position 4−16 in a 20-amino-acid residue (Figure S1); ζ-potential of the JTS-1 peptide (Figure S2); different interaction types of the peptide with MHC I alleles (Table S1); and different interaction types of the peptide with the MHC II alleles (Table S2) (PDF)

AUTHOR INFORMATION

Corresponding Author

Janakiraman Narayanan − *Department of Nanobiotechnology, Vision Research Foundation, Chennai, Tamil Nadu 600006, India;* ⓞ orcid.org/0000-0003-0866-9828; Phone: +91-44-28271616; Email: drjrn15@gmail.com; Fax: +91-44-28254180

Authors

Amit Chatterjee − *Department of Nanobiotechnology, Vision Research Foundation, Chennai, Tamil Nadu 600006, India*

Samdani Ansar − *Department of Bioinformatics, Vision Research Foundation, Chennai, Tamil Nadu 600006, India*

Divya Gopal − *Department of Nanobiotechnology, Vision Research Foundation, Chennai, Tamil Nadu 600006, India*

Umashankar Vetrivel − *Department of Bioinformatics, Vision Research Foundation, Chennai, Tamil Nadu 600006, India; Department of Health Research (Govt. of India), National Institute of Traditional Medicine, Indian Council of Medical Research, Belagavi 590010, India;* ⓞ orcid.org/0000-0003-4697-2115

Ronnie George − *Department of Glaucoma, Medical & Vision Research Foundation, Chennai, Tamil Nadu 600006, India*

Complete contact information is available at:
https://pubs.acs.org/10.1021/acsomega.2c00701

Notes

The authors declare no competing financial interest.

REFERENCES

(1) Xie, J.; Bi, Y.; Zhang, H.; Dong, S.; Teng, L.; Lee, R. J.; Yang, Z. Cell-Penetrating Peptides in Diagnosis and Treatment of Human Diseases: From Preclinical Research to Clinical Application. *Front. Pharmacol.* **2020**, *11*, No. 697.

(2) Chatterjee, A.; Nagarajan, H.; Padmanabhan, P.; Vetrivel, U.; Therese, K. L.; Janakiraman, N. Understanding the Uptake Mechanism and Interaction Potential of the Designed Peptide and Preparation of Composite Fiber Matrix for Fungal Keratitis. *ACS Omega* **2020**, *5*, 12090−12102.

(3) Amit, C.; Muralikumar, S.; Janaki, S.; Lakshmipathy, M.; Therese, K. L.; Umashankar, V.; Padmanabhan, P.; Narayanan, J. Designing and enhancing the antifungal activity of corneal specific cell penetrating peptide using gelatin hydrogel delivery system. *Int. J. Nanomed.* **2019**, *14*, 605−622.

(4) Lamb, H. M.; Wiseman, L. R. Pexiganan acetate. *Drugs* **1998**, *56*, 1047−1052.

(5) Mahlapuu, M.; Håkansson, J.; Ringstad, L.; Björn, C. Antimicrobial Peptides: An Emerging Category of Therapeutic Agents. *Front. Cell. Infect. Microbiol.* **2016**, *6*, No. 194.

(6) Tréhin, R.; Nielsen, H. M.; Jahnke, H.-G.; Krauss, U.; Beck-Sickinger, A. G.; Merkle, H. P. Metabolic cleavage of cell-penetrating peptides in contact with epithelial models: human calcitonin (hCT)-derived peptides, Tat(47-57) and penetratin(43-58). *Biochem. J.* **2004**, *382*, 945−956.

(7) Nguyen, L. H.; Gao, M.; Lin, J.; Wu, W.; Wang, J.; Chew, S. Y. Three-dimensional aligned nanofibers-hydrogel scaffold for controlled non-viral drug/gene delivery to direct axon regeneration in spinal cord injury treatment. *Sci. Rep.* **2017**, *7*, No. 42212.

(8) Fotin-Mleczek, M.; Welte, S.; Mader, O.; Duchardt, F.; Fischer, R.; Hufnagel, H.; Scheurich, P.; Brock, R. Cationic cell-penetrating peptides interfere with TNF signalling by induction of TNF receptor internalization. *J. Cell Sci.* **2005**, *118*, 3339−3351.

(9) Moschos, S. A.; Jones, S. W.; Perry, M. M.; Williams, A. E.; Erjefalt, J. S.; Turner, J. J.; Barnes, P. J.; Sproat, B. S.; Gait, M. J.; Lindsay, M. A. Lung delivery studies using siRNA conjugated to TAT(48-60) and penetratin reveal peptide induced reduction in gene expression and induction of innate immunity. *Bioconjugate Chem.* **2007**, *18*, 1450−1459.

(10) Ekokoski, E.; Aitio, O.; Törnquist, K.; Yli-Kauhaluoma, J.; Tuominen, R. K. HIV-1 Tat-peptide inhibits protein kinase C and protein kinase A through substrate competition. *Eur. J. Pharm. Sci.* **2010**, *40*, 404−411.

(11) Ganju, R. K.; Munshi, N.; Nair, B. C.; Liu, Z. Y.; Gill, P.; Groopman, J. E. Human immunodeficiency virus tat modulates the Flk-1/KDR receptor, mitogen-activated protein kinases, and components of focal adhesion in Kaposi's sarcoma cells. *J. Virol.* **1998**, *72*, 6131−6137.

(12) Gottschalk, S.; Sparrow, J. T.; Hauer, J.; Mims, M. P.; Leland, F. E.; Woo, S. L.; Smith, L. C. A novel DNA-peptide complex for efficient gene transfer and expression in mammalian cells. *Gene Ther.* **1996**, *3*, 448−457.

(13) Erazo-Oliveras, A.; Muthukrishnan, N.; Baker, R.; Wang, T.-Y.; Pellois, J.-P. Improving the endosomal escape of cell-penetrating peptides and their cargos: strategies and challenges. *Pharmaceuticals* **2012**, *5*, 1177−1209.

(14) Amit, C.; Padmanabhan, P.; Elchuri, S. V.; Narayanan, J. Probing the effect of matrix stiffness in endocytic signalling pathway of corneal epithelium. *Biochem. Biophys. Res. Commun.* **2020**, *525*, 280−285.

(15) Mouneimne, G.; Hansen, S. D.; Selfors, L. M.; Petrak, L.; Hickey, M. M.; Gallegos, L. L.; Simpson, K. J.; Lim, J.; Gertler, F. B.; Hartwig, J. H.; et al. Differential remodeling of actin cytoskeleton architecture by profilin isoforms leads to distinct effects on cell migration and invasion. *Cancer Cell* **2012**, *22*, 615−630.

(16) Yamanaka, O.; Kitano-Izutani, A.; Tomoyose, K.; Reinach, P. S. Pathobiology of wound healing after glaucoma filtration surgery. *BMC Ophthalmol.* **2015**, *15*, No. 157.

(17) Conlon, R.; Saheb, H.; Ahmed, I. I. K. Glaucoma treatment trends: a review. *Can. J. Ophthalmol.* **2017**, *52*, 114−124.

(18) Rulli, E.; Biagioli, E.; Riva, I.; Gambirasio, G.; De Simone, I.; Floriani, I.; Quaranta, L. Efficacy and safety of trabeculectomy vs nonpenetrating surgical procedures: a systematic review and meta-analysis. *JAMA Ophthalmol.* **2013**, *131*, 1573−1582.

(19) Salim, S. Current variations of glaucoma filtration surgery. *Curr. Opin. Ophthalmol.* **2012**, *23*, 89−95.

(20) Nakamura-Shibasaki, M.; Ko, J.-A.; Takenaka, J.; Chikama, T.-I.; Sonoda, K.-H.; Kiuchi, Y. Matrix metalloproteinase and cytokine expression in Tenon fibroblasts during scar formation after glaucoma filtration or implant surgery in rats. *Cell Biochem. Funct.* **2013**, *31*, 482−488.

(21) Wang, J.; Harris, A.; Prendes, M. A.; Alshawa, L.; Gross, J. C.; Wentz, S. M.; Rao, A. B.; Kim, N. J.; Synder, A.; Siesky, B. Targeting Transforming Growth Factor-*β* Signaling in Primary Open-Angle Glaucoma. *J. Glaucoma* **2017**, *26*, 390−395.

(22) Trelford, C. B.; Denstedt, J. T.; Armstrong, J. J.; Hutnik, C. M. L. The Pro-Fibrotic Behavior of Human Tenon's Capsule Fibroblasts in Medically Treated Glaucoma Patients. *Clin. Ophthalmol.* **2020**, *14*, 1391−1402.

(23) Mietz, H.; Krieglstein, G. K. Postoperative application of mitomycin c improves the complete success rate of primary trabeculectomy: a prospective, randomized trial. *Graefe's Arch. Clin. Exp. Ophthalmol.* **2006**, *244*, 1429−1436.

(24) Cabourne, E.; Clarke, J. C. K.; Schlottmann, P. G.; Evans, J. R. Mitomycin C versus 5-Fluorouracil for wound healing in glaucoma surgery. *Cochrane Database Syst. Rev.* **2015**, *2015*, No. CD006259.

(25) Hong, S.; Han, S.-H.; Kim, C. Y.; Kim, K. Y.; Song, Y. K.; Seong, G. J. Brimonidine reduces TGF-beta-induced extracellular matrix synthesis in human Tenon's fibroblasts. *BMC Ophthalmol.* **2015**, *15*, No. 54.

(26) Garnock-Jones, K. P. Ripasudil: first global approval. *Drugs* **2014**, *74*, 2211−2215.

(27) Lee, D. A.; Hersh, P.; Kersten, D.; Melamed, S. Complications of subconjunctival 5-fluorouracil following glaucoma filtering surgery. *Ophthalmic Surg., Lasers Imaging Retina* **1987**, *18*, 187−190.

(28) Larsen, M. V.; Lundegaard, C.; Lamberth, K.; Buus, S.; Lund, O.; Nielsen, M. Large-scale validation of methods for cytotoxic T-lymphocyte epitope prediction. *BMC Bioinf.* **2007**, *8*, No. 424.

(29) Jensen, K. K.; Andreatta, M.; Marcatili, P.; Buus, S.; Greenbaum, J. A.; Yan, Z.; Sette, A.; Peters, B.; Nielsen, M. Improved methods for predicting peptide binding affinity to MHC class II molecules. *Immunology* **2018**, *154*, 394−406.

(30) e Oliveira, D. M. T.; de Serpa Brandão, R. M. S.; da Mata Sousa, L. C. D.; das Chagas Alves Lima, F.; do Monte, S. J. H.; Marroquim, M. S. C.; de Sousa Lima, A. V.; Coelho, A. G. B.; Costa, J. M. S.; Ramos, R. M.; da Silva, A. S. pHLA3D: An online database of predicted three-dimensional structures of HLA molecules. *Hum. Immunol.* **2019**, *80*, 834−841.

(31) Zhou, P.; Jin, B.; Li, H.; Huang, S.-Y. HPEPDOCK: a web server for blind peptide-protein docking based on a hierarchical algorithm. *Nucleic Acids Res.* **2018**, *46*, W443−W450.

(32) Zhou, P.; Li, B.; Yan, Y.; Jin, B.; Wang, L.; Huang, S.-Y. Hierarchical Flexible Peptide Docking by Conformer Generation and Ensemble Docking of Peptides. *J. Chem. Inf. Model.* **2018**, *58*, 1292−1302.

(33) Lock, J. G.; Stow, J. L. Rab11 in recycling endosomes regulates the sorting and basolateral transport of E-cadherin. *Mol. Biol. Cell* **2005**, *16*, 1744−1755.

(34) Campos, S. B.; Ashworth, S. L.; Wean, S.; Hosford, M.; Sandoval, R. M.; Hallett, M. A.; Atkinson, S. J.; Molitoris, B. A. Cytokine-induced F-actin reorganization in endothelial cells involves RhoA activation. *Am. J. Physiol.: Renal Physiol.* **2009**, *296*, F487−F495.

(35) Huang, Y.; Jiang, Y.; Wang, H.; Wang, J.; Shin, M. C.; Byun, Y.; He, H.; Liang, Y.; Yang, V. C. Curb challenges of the "Trojan Horse" approach: smart strategies in achieving effective yet safe cell-penetrating peptide-based drug delivery. *Adv. Drug Delivery Rev.* **2013**, *65*, 1299−1315.

(36) Habault, J.; Poyet, J.-L. Recent Advances in Cell Penetrating Peptide-Based Anticancer Therapies. *Molecules* **2019**, *24*, No. 927.

(37) Shigenaga, A.; Yamamoto, J.; Kohiki, T.; Inokuma, T.; Otaka, A. Invention of stimulus-responsive peptide-bond-cleaving residue (Spr) and its application to chemical biology tools. *J. Pept. Sci.* **2017**, *23*, 505−513.

(38) Vaysse, L. Improved transfection using epithelial cell line-selected ligands and fusogenic peptides. *Biochim. Biophys. Acta, Gen. Subj.* **2000**, *1475*, 369−376.

(39) Rittner, K.; Benavente, A.; Bompard-Sorlet, A.; Heitz, F.; Divita, G.; Brasseur, R.; Jacobs, E. New basic membrane-destabilizing peptides for plasmid-based gene delivery in vitro and in vivo. *Mol. Ther.* **2002**, *5*, 104−114.

(40) Brugnano, J.; McMasters, J.; Panitch, A. Characterization of endocytic uptake of MK2-inhibitor peptides. *J. Pept. Sci.* **2013**, *19*, 629−638.

(41) Kilchrist, K. V.; Evans, B. C.; Brophy, C. M.; Duvall, C. L. Mechanism of Enhanced Cellular Uptake and Cytosolic Retention of MK2 Inhibitory Peptide Nano-polyplexes. *Cell. Mol. Bioeng.* **2016**, *9*, 368−381.

(42) Tai, W.; Gao, X. Functional peptides for siRNA delivery. *Adv. Drug Delivery Rev.* **2017**, *110−111*, 157−168.

(43) Bastin, G.; Heximer, S. P. Rab family proteins regulate the endosomal trafficking and function of RGS4. *J. Biol. Chem.* **2013**, *288*, 21836−21849.

(44) Grant, B. D.; Donaldson, J. G. Pathways and mechanisms of endocytic recycling. *Nat. Rev. Mol. Cell Biol.* **2009**, *10*, 597−608.

(45) Wandinger-Ness, A.; Zerial, M. Rab proteins and the compartmentalization of the endosomal system. *Cold Spring Harbor Perspect. Biol.* **2014**, *6*, No. a022616.

(46) Bertram, E. M.; Hawley, R. G.; Watts, T. H. Overexpression of rab7 enhances the kinetics of antigen processing and presentation with MHC class II molecules in B cells. *Int. Immunol.* **2002**, *14*, 309−318.

(47) Montealegre, S.; van Endert, P. M. Endocytic Recycling of MHC Class I Molecules in Non-professional Antigen Presenting and Dendritic Cells. *Front. Immunol.* **2019**, *9*, No. 3098.

(48) Chaplin, D. D. Overview of the immune response. *J. Allergy Clin. Immunol.* **2010**, *125*, S3−S23.

(49) Wieczorek, M.; Abualrous, E. T.; Sticht, J.; Álvaro-Benito, M.; Stolzenberg, S.; Noé, F.; Freund, C. Major Histocompatibility Complex (MHC) Class I and MHC Class II Proteins: Conformational Plasticity in Antigen Presentation. *Front. Immunol.* **2017**, *8*, No. 292.

(50) Cho, K.-J.; Ishido, S.; Eisenlohr, L. C.; Roche, P. A. Activation of Dendritic Cells Alters the Mechanism of MHC Class II Antigen Presentation to CD4 T Cells. *J. Immunol.* **2020**, *204*, 1621−1629.

(51) Doi, M.; Shichiri, M.; Katsuyama, K.; Marumo, F.; Hirata, Y. Cytokine-activated p42/p44 MAP kinase is involved in inducible nitric oxide synthase gene expression independent from NF-kappaB activation in vascular smooth muscle cells. *Hypertens. Res.* **2000**, *23*, 659−667.

(52) Tanihara, H.; Inoue, T.; Yamamoto, T.; Kuwayama, Y.; Abe, H.; Araie, M. Phase 2 randomized clinical study of a Rho kinase inhibitor, K-115, in primary open-angle glaucoma and ocular hypertension. *Am. J. Ophthalmol.* **2013**, *156*, 731−736.